

Structural
assessment
of POAG



OCT and
automated
perimetry
interpretation
explained



How can structural
and functional
data be combined
to help diagnosis
and management
of disease

Functional
assessment
of POAG

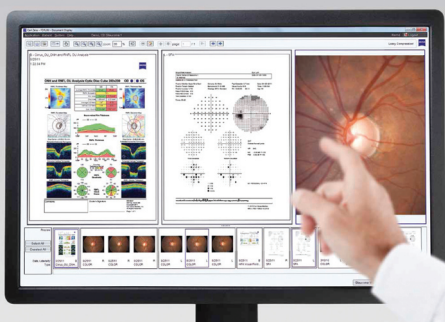


Optician

The weekly journal for eye care professionals | opticianonline.com

12.09 & 17.10.2014

1. Capture



2. Review



3. Decide



ZEISS FORUM glaucoma

Know when to intervene



www.zeiss.co.uk 01223 401 450 customercare.uk@zeiss.com

We make it visible.



The future is here: Structural and functional assessment of primary open-angle glaucoma

Part 1 Structure

Primarily open-angle glaucoma can be considered as a member of the family of diseases that exhibit an optic neuropathy which is characterised by progressive neuroretinal rim thinning and excavation, manifested as a loss of the retinal ganglion cells in the inner retina and their axons in the retinal nerve fibre layer (RNFL) and a deformation of connective tissues supporting the optic nerve head, together with a corresponding visual field defect.¹⁻²

While the definition of primary open-angle glaucoma has not materially changed in recent years, the sophistication of the investigative techniques used for the detection and management of glaucoma is currently moving at an unprecedented pace with the advent of *in-vivo* high resolution imaging using spectral domain (and other modes of) optical coherence tomography (OCT). Such advances are not only resulting in the detection of glaucoma at an earlier stage but are also aiding the understanding of the disease process, itself. In parallel with the developments in OCT, is the re-alignment of the importance of the visual field examination using standard automated perimetry.³⁻⁵

It should be stressed that the definition of primary open-angle glaucoma includes measures of both structure and function, ie, both assume equal importance in the detection and assessment of the disease. In the early stages of primary open-angle glaucoma, abnormalities of structure and function can occur concurrently in some patients, while other patients seemingly manifest detectable abnormality of one modality prior to the other. In addition, there can be considerable variation between the structural appearance and the functional outcome across individuals.

The advantage of high resolution imaging, together with the associated quantitative capability, is obvious in the characterisation of the optic nerve head and of the RNFL, but such techniques

In the first of two articles offering an update on the detection and assessment of structural and functional abnormality in primary open-angle glaucoma, **Professor John Wild** focuses on the use of OCT.

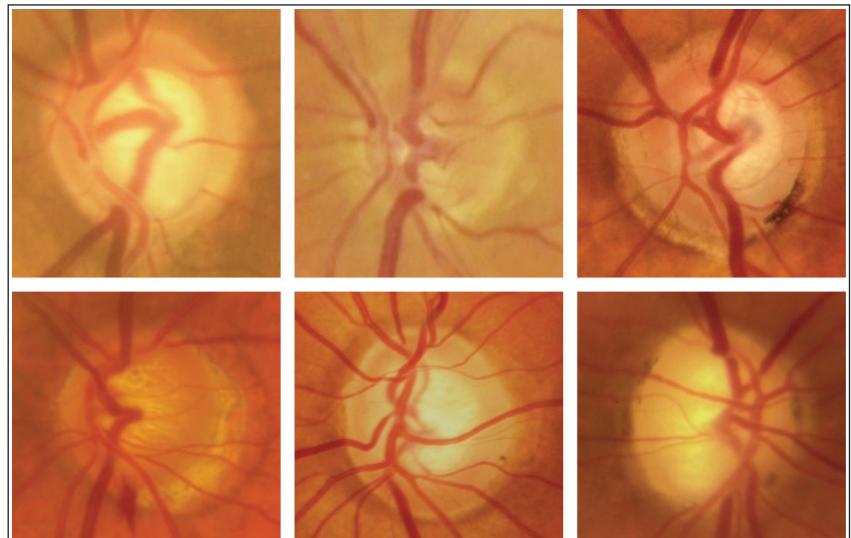


Figure 1 Characteristic appearances of glaucomatous optic neuropathy

are also enabling an evaluation of the retinal ganglion cell layer and of the lamina cribrosa.

This article will review the 'best/preferred practice' approach to the detection of primary open-angle glaucoma with particular emphasis on the evaluation of structural and functional integrity. The interpretation of the OCT printout will then be discussed. This will cover spectral domain OCT of the optic nerve head, of the peripapillary RNFL and of the retinal ganglion cell layer/inner plexiform layer complex. In Part 2, standard automated perimetry will be covered and the utility of a combined structural and functional approach to the examination of patients with glaucoma will be illustrated.

The characteristics of the optic nerve head associated with primary open-angle glaucoma are long established and include an increase in cup size, an increase in cup to disc ratio, disc asymmetry, changes in the lamina

cribrosa, loss of neuroretinal rim, pallor, increase in peripapillary atrophy, vessel changes and disc margin haemorrhage⁶ (Figure 1). Such appearances are best viewed stereoscopically and both the qualitative and quantitative documentation depend upon the skill of the clinician. The associated abnormality of the RNFL has traditionally received less attention but can be documented by red-free viewing (Figure 2).

Spectral domain optical coherence tomography

Optical coherence tomography is an objective non-invasive *in-vivo* three-dimensional imaging technique which uses the principle of low-coherence interferometry to image the light backscattered from a given structure. For ocular investigation, the light source is a broadband superluminescent diode, generally centred at 840nm. Light from the diode is split into two optical beams. The sample beam is scanned across the given structure and



the reference beam travels to a mirror. The returning beams are recombined at a detector which, in the case of spectral domain (also known as Fourier domain) OCT, is a spectrometer. The relative amplitudes and phases of the spectral components of the recombined light returning from throughout the depth of the structure under investigation are then processed using Fourier analysis. The required sequence of one-dimensional depth scanning (A-scans) form a series of B-scans that generate a three-dimensional image of the given structure. Current generation clinical spectral domain OCT systems can acquire approximately 25,000 to 40,000 A-scans per second. The axial resolution of spectral domain OCT is between 5 and 10 μ m.

OCT was initially applied in eye care for the investigation of vitreo-retinal and macular disease. However, the technique has now also radically altered the approach/emphasis to the detection and management of glaucoma. It enables quantitative measures not only of the optic nerve head but also of the peripapillary RNFL thickness and of the combined macular ganglion cell/inner plexiform layer complex thickness. These measures are then compared to age- and/or disc size-corrected normal values. The assessment of the macular ganglion cell/inner plexiform layer complex thickness in glaucoma is currently the subject of much research interest.⁷⁻⁸

For imaging the optic nerve head with the Cirrus HD-OCT (Figure 3), for example, a 6mm by 6mm data cube is generated from a series of 200 B-scans, each composed of 200 A-scans. The disc edge is defined as the termination of Bruch's membrane and the neuro-retinal rim width is determined by direct measurement of the neural tissue in the nerve head. By such means, the disc and rim area measurements correspond closely to the anatomy in the same plane as the nerve head and this approach also overcomes the distortion of the image which occurs when viewing a tilted disc. Software within the instrument then identifies the centre of the optic nerve head and evaluates the RNFL thickness along a 256 A-scan 3.46 mm diameter circle around the nerve head. When misalignment of the data cube occurs, the RNFL circle analysis is automatically corrected by the instrument software. Similarly, the thickness of the macular ganglion cell layer/inner plexiform layer complex is derived from one of two corresponding macular 6mm by 6mm cube scans (128 B-scans each composed of 512 A-scans

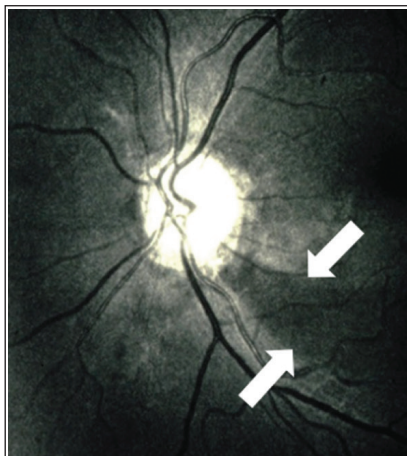


Figure 2 An inferior-temporal RNFL defect in the left eye visible by red-free illumination. The defect is indicated between the white arrows. Note, in contrast, the visibility of the normal RNFL entering the superior pole of the nerve head



Figure 3 The Cirrus HD-OCT 500

and 200 B-scans each composed of 200 A-scans, respectively).

Standard automated perimetry

The most sensitive measure of the visual field is standard automated perimetry, ie, threshold perimetry generally using a white Goldmann size III stimulus presented on a white background of 10cdm⁻² luminance.

Threshold perimetry estimates the differential light threshold, the minimum luminance (brightness), ΔL , of the stimulus necessary to evoke a response presented against a background of given constant luminance, L . The output at each stimulus location is expressed in terms of the reciprocal of the threshold, $\Delta L/L$, the differential light sensitivity. The unit of measurement is the decibel (dB) where 0dB represents the maximum luminance of the stimulus and 1 dB is equivalent to a 0.1 log unit reduction in the stimulus luminance.

In the early 1990s, a number of studies suggested that between 25 per cent and 50 per cent of the retinal ganglion cells in primary open-angle glaucoma could be damaged before the manifestation of a visual field defect and that ganglion cell axons with larger diameter were preferentially damaged in glaucoma.⁹ This finding led to the development of alternative techniques of perimetry which purported to 'target' sub-populations of retinal ganglion cells which were either preferentially damaged by the glaucoma process or exhibited lower degrees of overlap between adjacent receptive fields and would, therefore, demonstrate functional deficits earlier in the disease

process since only a small number of cells would need to be lost prior to the loss of adequate retinal receptive field coverage.¹⁰ Such commercially available techniques of perimetry included Frequency Doubling Technology perimetry, short-wavelength automated perimetry, luminance pedestal flicker perimetry and critical fusion flicker perimetry. However, there is no clear evidence base to suggest that any of these alternative techniques determines visual field loss in advance of that by standard automated perimetry. Indeed, it is now accepted that the initial findings relating ganglion cell numbers to perimetric output were a consequence of the inadequacy of the histological process,¹¹ of an initial comparison with the results of kinetic perimetry, and of a subsequent comparison with the results of threshold perimetry considered in dB¹²

The dB scale is logarithmic and, by definition, identical dB increments or decrements at different levels of sensitivity represent different increments or decrements of luminance when considered on a linear scale. Thus, the true nature of the structure and function relationship was initially confounded by the comparison of retinal ganglion cell count in linear units and the visual field outcome in logarithmic units. Such a comparison exhibits a curvilinear relationship which suggests, inadvertently, that, in early disease, structural damage is greater than functional damage and that, in more severe disease, functional damage declines at a greater rate than structural damage. However, when the two measures are considered on the same measurement scales, ie logarithmic against logarithmic plots or linear against linear plots, the relationship between differential light sensitivity and ganglion cell number, and also other measures such as rim area, is ►

linear over the abnormal range, at least. Indeed, it is now recognised that there is an almost one-to-one relationship between the number of ganglion cell soma calculated from standard automated perimetry and the number of ganglion cell axons calculated from OCT¹³⁻¹⁴ (Figure 4).

The OCT printout for the optic nerve head and the RNFL characteristics generally presents quantitative measures displayed on a background colour which is coded for the statistical probability of the likelihood of the measured value lying within the age- and/or disc size/area-corrected normal range. Green indicates normality and yellow and red indicate abnormality at the p<5 per cent and p<1 per cent probability level, respectively. In addition, the print-out also generally displays two-dimensional B-scans of the optic nerve head and of the RNFL. The print-out for OCT generally contains the recording for both eyes.

A useful mnemonic for the interpretation of the OCT printout is WANDER. This was originally developed for the interpretation of the visual field printout but can be also applied to that from OCT, ie, **W**hat was done; **A**re the results **A**ccurate/**A**dequate; **N**ormal; if no, what type of **D**efect is present; **E**valuate the type of defect (ie is it compatible with the signs and symptoms); **R**e-evaluate the defect (ie has it worsened)?

Interpretation of the RNFL and Optic Nerve Head Analysis Report

The components of the printout for the RNFL and optic nerve head analysis report for the Cirrus HD-OCT are illustrated in Figure 5 but are applicable to most types of spectral domain OCT systems.

What was done?

This question refers to such factors as the given number and orientation of the A-scans forming the given number of B-scans of the given image, eg, the 200 by 200 optic disc cube (1), as highlighted in Figure 5.

Are the results **Accurate/ Adequate**? With the Cirrus HD-OCT, the adequacy of the image is quantified by the signal strength which is measured on an integer scale from 0 to 10. The minimum acceptable signal strength is 6; however, a value of at least 7 or 8 is desirable.

After segmentation, the delineation of the layers in each B-scan image should be interrogated for the presence of errors whereby the image data is such

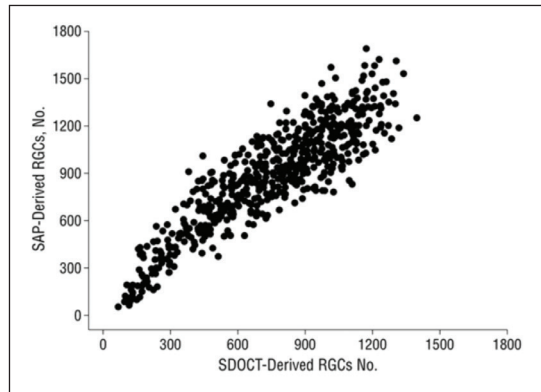


Figure 4 Scatterplot illustrating the relationship between the number of retinal ganglion cells (RGCs) derived from standard automated perimetry (SAP) and the number of RGCs estimated from analysis of the RNFL by spectral domain optical coherence tomography (SDOCT)

that the instrument software is unable to differentiate, correctly, the various retinal layers either across the complete scan or in a localised region. Such errors may arise from epiretinal membranes and posterior vitreous detachments, with posterior staphyloma, and with

extensive peripapillary atrophy, but may also be caused by gross movements of the patient during the image acquisition.

The printout should also be interpreted with caution in the presence of posterior subcapsular and cortical cataract, which can lead to a reduction in the image quality.

The lateral dimensions of the en-face image are dependent upon the axial length of the eye. As an OCT instrument uses an average axial length, the lateral dimensions of the image may be over- or under-estimated in excessively shorter and longer eyes, respectively.

Is the scan **Normal**?

If a **Defect** is present, what type of **Defect** is it?

Evaluate the type of **Defect**. Is it compatible with the signs and symptoms of the patient?

Quantitative measures of the optic nerve head parameters

The quantitative measures of the rim and disc area, the vertical cup-to-disc ratio and the cup volume (2) for

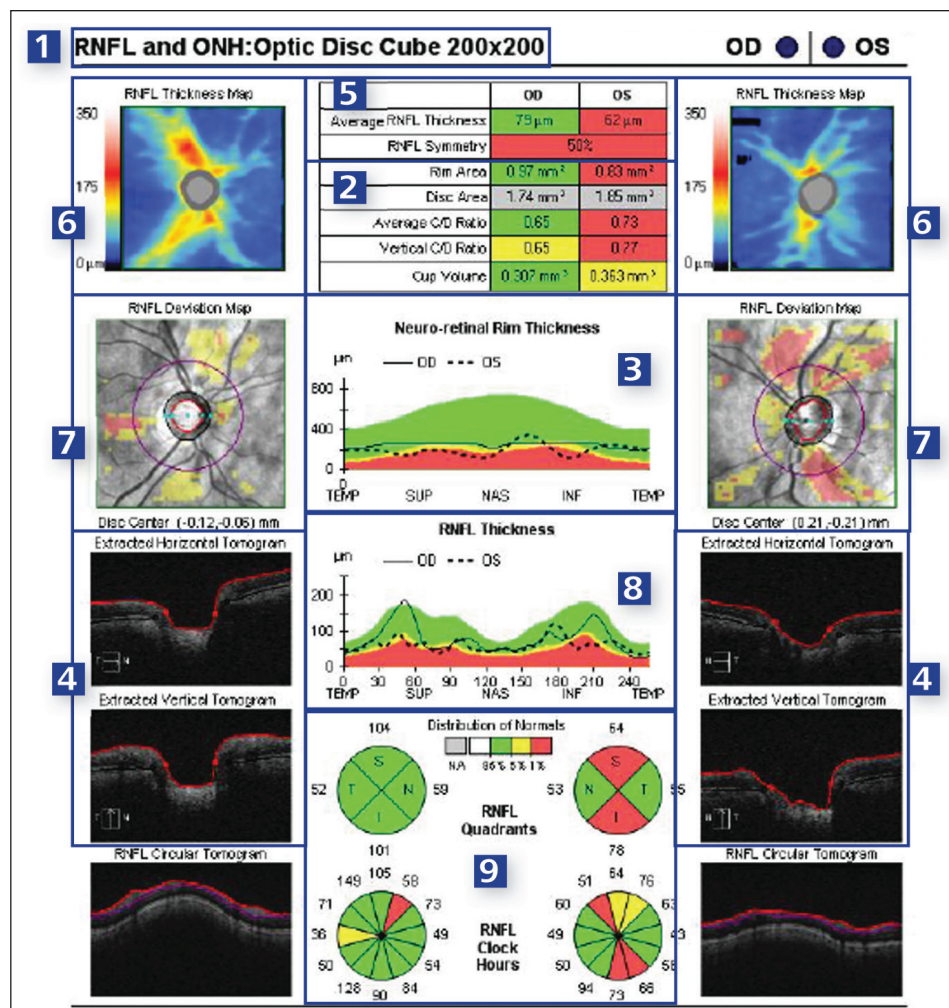


Figure 5 The printout for the RNFL and optic nerve head characteristics derived using the 200x200 Optic Disc Cube of the Cirrus HD-OCT 500

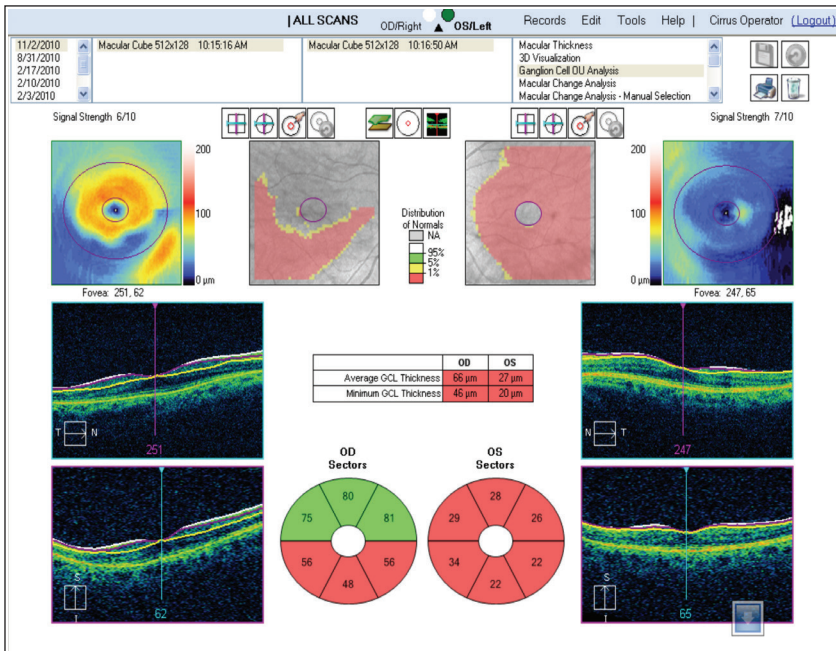


Figure 6 The printout for the ganglion cell/ inner plexiform layer complex thickness derived using the 512x128 Macular Cube of the Cirrus HD-OCT 500

each eye and between-eyes should be evaluated in the context of the qualitative impression of the optic nerve head obtained from slit lamp binocular indirect ophthalmoscopy. In the case of the Cirrus HD-OCT, these quantitative values are corrected for age and nerve head area; as a consequence, the disc area is not associated with any given statistical probability value. If the disc area is either smaller than 1.3mm² or greater than 2.5mm², respectively, a probability value for the remaining optic nerve head parameters cannot be calculated due to insufficient numbers of individuals within the normative data base manifesting such values. The range of normality for the vertical cup-to-disc ratio is surprisingly wide: in the case of a 69-year-old, for example, the normal range lies between 0.21 and 0.64.

Neuro-retinal Rim Thickness profile
The above values should also be compared with the Neuro-retinal Rim Thickness graph (3).

The Neuro-retinal Rim Thickness profile schematically displays, simultaneously in each eye, the neuro-retinal rim thickness at any given angular location referenced to the statistical likelihood of the value lying within the age- and disc area-corrected normal range.

The B-scan display (4) provides useful additional qualitative information not only of the depth of the cup but also of the corresponding slope of the cup walls; however, such information is not coded for probability level.

Quantitative measures of the RNFL thickness

The remaining part of the printout is heavily weighted towards the interpretation of the RNFL Thickness. The Average RNFL Thickness (5) is corrected for age, only, and should be evaluated in the context of the corresponding disc size. Small and large discs will exhibit thinner and thicker peripapillary RNFL thicknesses, respectively, than the average size disc since the 3.46 mm diameter circle along which the measurement is made will be further from or nearer to, respectively, the maximum RNFL thickness.

The en-face RNFL Thickness map

The en-face RNFL thickness map (ie the 'straight ahead view' of the RNFL as 'seen' by the clinician through the pupil) (6) is illustrated by false colours whereby red and other warm colours represent thicker values and cold colours represent thinner values with blue representing the thinnest values. The thickness map is analogous to the grey scale of perimetry; however, the shading of both maps is not corrected for age- or eccentricity-related normal variations in either thickness or sensitivity, respectively. The en-face thickness map in the normal eye should comprise warm colours, which become increasingly warmer as the vertical poles of the optic nerve head are approached, and represents the convergence towards, and entry into, the nerve head of the majority of the retinal ganglion cell axons.

The en-face RNFL Deviation map (7) illustrates the statistical probability of the given deviation lying within the normal range and the probability level is colour coded in yellow (<5 per cent) or red (<1 per cent) against a grey background. The RNFL Deviation map is analogous to the Total Deviation Probability map for perimetry (see Part 2) and evaluates overall/generalised changes in the thickness of the RNFL.

The RNFL Thickness 'TISNT' graph

The 'TISNT' graph (8) schematically displays, simultaneously in each eye, the peripapillary retinal nerve fibre thickness, 'unravell'd from the 3.46 mm diameter circle, in a profile format continuously from the horizontal temporal meridian to the superior, nasal and inferior meridians and back to the horizontal temporal meridian. The values are also referenced to the statistical likelihood of the given value at the given eccentricity lying within the age-corrected normal range.

The RNFL Quadrant and Clock Hours average thickness pie charts

The average peripapillary RNFL thickness for each of the four quadrants, defined by the oblique meridia, and for each of 12 equal sectors (9) are referenced to the statistical likelihood of the value lying within the age-corrected normal range.

Case Number 1

The patient in Figure 5 has primary open-angle glaucoma in the left eye and is a glaucoma suspect in the right eye. He exhibits, in the left eye, abnormal vertical and average cup-to-disc ratios (p<0.01 and p<0.01, respectively), an abnormal neuro-retinal rim area (p<0.01) and an abnormal cup volume (p<0.05) (2). In the right eye, the vertical cup-to-disc ratio, only, lies outside the normal range (p<0.05) (2). The Neuro-retinal Rim Thickness profile indicates that the rim thickness of the left nerve head exhibits focal thinning which is outside the normal range particularly superiorly but also inferiorly (3). The rim thickness is borderline normal in the right eye. The corresponding B-scans (4) show the extent of, and the difference in, the enlargement of the cup between the meridians and between eyes. The magnitude of the cup and the variations in the slope of the cup wall are particularly evident for the left eye. As might be expected from the characteristics of the left optic nerve head, the average RNFL thickness is outside the normal range (5) and is ►

statistically thinner in the left eye than in the right eye. The RNFL Thickness Map (6) exhibits an absence of 'warm' colours at the superior and inferior poles of the left optic nerve head indicating a thinning of the RNFL in these regions. The red colour in the RNFL Deviation Map (7) indicates that the thickness of the RNFL in these regions lies outside of the normal range ($p < 0.01$). In the right eye, the RNFL Deviation Map suggests a thinning of the RNFL in the papillo-macular region.

Thus, the information for the left eye, so far, indicates a predominantly vertically increased cup, with a consequent reduction in the neuro-retinal rim thickness and RNFL Thickness, both superiorly and inferiorly.

As would be expected from the above, the RNFL Thickness 'TISNT' graph (8) for the left eye exhibits superior and inferior nerve fibre layer thicknesses which are abnormally thin ($p < 0.01$ and $p < 0.01$, respectively). The RNFL Quadrant and Clock Hours (9) average thickness pie charts confirm the thinning at the superior and inferior poles. The thinning covers three sectors superiorly, two of which are at a probability level of $p < 0.05$, while that inferiorly covers two sectors both of which are at a probability level of $p < 0.01$. The values for the right eye would generally appear to lie within the normal range. The RNFL thickness in the right eye at the 9 o'clock sector (ie that which corresponds to the papillomacular bundle) is abnormal at the 5 per cent level and is a further illustration of the information displayed in the RNFL Deviation Map (7). Such an outcome is suspicious and requires follow-up.

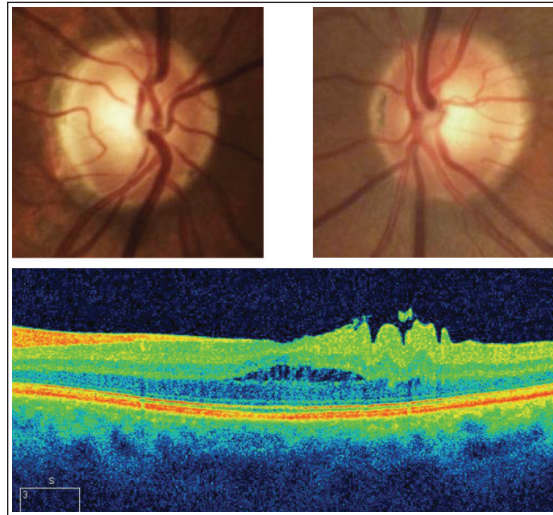


Figure 7a The optic nerve head images and OCT B scan for a patient under review for ocular hypertension

Caution should be exercised in the context of what is becoming known as 'red disease' which is, essentially, a false-positive outcome, ie, the occurrence of an abnormality due to chance. Such an eventually is known statistically as a Type I error: assuming a probability level of 5 per cent, such an error will occur five times in every 100 statistical comparisons. Conversely, the opposite, 'green disease' can also occur whereby manifest disease is not detected by the statistical process. In addition, the various measures co-vary, eg, an increased cup is associated with a reduced neuro-retinal rim. Accordingly, it essential that the clinician has a sound knowledge of the various statistical outputs and 'integrates' the information with other clinical signs and with the symptoms.

Interpretation of the Ganglion Cell Analysis Report

The printout for the Ganglion Cell

Analysis Report derived from the 512 by 128 macular cube is illustrated in Figure 6 for a patient with primary open-angle glaucoma. The components of the print-out are based upon the same concepts as the print-out for the optic nerve head and RNFL thickness analyses. The patient in Figure 6 exhibits a gross reduction in the ganglion cell/inner plexiform layer thickness complex of each eye, as evidenced by the thickness maps, the deviation maps and the sectorial maps which are more pronounced for the left eye.

Case Number 2

An interesting case is presented in Figure 7. The patient was being followed as an ocular hypertensive. At the most recent visit the peripapillary RNFL thickness of both eyes was within the normal range. However, the patient was found to have developed a lamellae macular hole in the left eye together with an epiretinal membrane. The visual acuity in the left eye was 6/7.5. Interestingly the ganglion cell/inner plexiform layer thickness complex was grossly abnormal in both eyes and was indicative of primary open-angle glaucoma. ●

● In Part 2, the author will discuss the interpretation of standard automated perimetry and look at how combined OCT and perimetric probability analyses represents a significant stride forward in the health assessment of the eye.

● **Professor John Wild** is Professor of Clinical Vision Sciences at Cardiff University and Honorary Research Fellow at the University Hospital of Wales

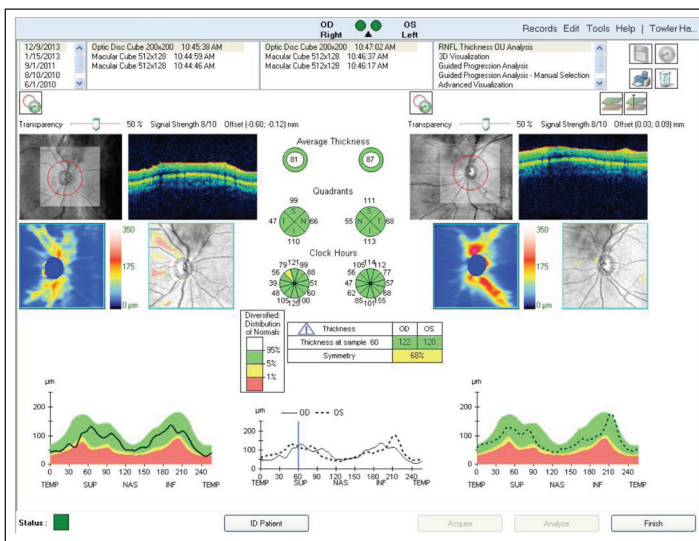


Figure 7b Normal peripapillary RNFL thickness in each eye for the patient under review for ocular hypertension

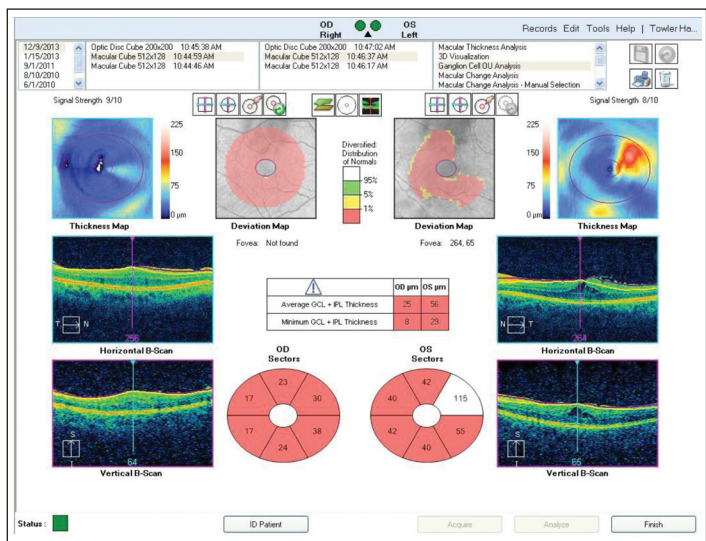


Figure 7c Severe attenuation of the ganglion cell/inner plexiform layer thickness in each eye, with the greater reduction in the right eye, for the patient under review for ocular hypertension



The future is here: Structural and functional assessment of primary open-angle glaucoma

Part 2 - Function

Part 1 of this article (*Optician* 12.09.14) reprised the relationship between structural and functional outcomes in primary open-angle glaucoma. It then discussed the interpretation of the optic nerve head features and of the thicknesses of the retinal nerve fibre layer and of the macular ganglion cell/ inner plexiform layer complex, respectively, derived by optical coherence tomography (OCT). In the final part of this article, the interpretation of the visual field printout will be discussed, and an insight will be given into the utility of combined structural and functional probability analyses in the diagnosis and management of primary open-angle glaucoma.

Interpretation of the visual field printout

The components of the printout are illustrated for the Humphrey Field Analyzer (HFA) in Figure 8 but are applicable to most types of perimeter.

What was done?

This question refers to the stimulus program (the array of stimulus locations to be examined), eg Program 24-2; to the stimulus size (the default is usually Goldmann size III which subtends an angle of 0.431° at the eye); to the threshold algorithm (the sequence of stimulus luminances by which an estimate of threshold is obtained), eg SITA Fast; and to other details such as the refractive correction used (1). The background luminance for most perimeters is generally not changeable and, as was stated in Part 1 of this article, is normally 10cdm^{-2} (31.5asb).

Are the results Accurate/Adequate?

This question refers to the number of incorrect responses to each of the two sets of reliability parameters, the false-positive and the false-negative catch trials, and to the number of fixation losses detected by the Heijl-Krakau blind spot technique (2).

The false-positive catch trials are generated by the perimeter occasionally purporting to present a stimulus. If the

patient apparently 'sees' the stimulus, a false-positive response is recorded. A rate of false-positive responses of >20 per cent of the total number of apparent presentations indicates an unreliable test result due to a 'trigger-happy' or 'jumping the gun' patient. With the SITA algorithms of the HFA, a false-positive response is deemed to have occurred if the patient responds either within a designated period, based upon their own response times for 'true' responses, from the appearance of the stimulus, or after a fixed time following disappearance of the stimulus, or both.¹⁵ With this latter approach, which supersedes the

earlier method and slightly shortens the duration of the examination, false-positive responses of >15 per cent can be considered to constitute an unreliable result. The false-negative catch trials are generated by the presentation of a stimulus at a given location which is brighter than the sensitivity recorded earlier in the examination. If the patient fails to see the stimulus, a false-negative response is recorded. An incorrect response rate of >33 per cent of the total number of false-negative catch trial presentations has traditionally been used to indicate an unreliable test result. However, an 'unacceptably' high proportion of false-negative responses occurring progressively towards the end of the examination indicates a fatigue effect. Equally so, an 'unacceptably' high proportion of false-negative responses can be physiologically associated with moderate to severe damage to the visual field and arises from the inherent increased variability associated with the reduced sensitivity at the given stimulus location.¹⁶

Fixation loss catch trials are generated by the presentation of a stimulus into the physiological blind spot. If a patient responds to the stimulus, a fixation loss is recorded. If the incorrect responses are >20 per cent or >30 per cent (depending upon the authority) of the total number of stimulus presentations within the blind spot, the test results are deemed to be unreliable. With the HFA, approximately 5 per cent of the total number of stimulus presentations are presented within the blind spot. An alternative approach to the Heijl-Krakau technique is to utilise gaze tracking (available on the HFA 740i and above) whereby an infrared source is imaged on the pupil centre. The distance between the pupil centre and the first Purkinje image is tracked throughout the examination. An eye movement ▶

Figure 8 Single field printout of the visual field recorded with the SITA Fast algorithm and Program 24-2 of the Humphrey Field Analyzer (HFA) for the left eye of a patient with a nuclear cataract and glaucoma. Note the difference in the appearance of the Total and Pattern Deviation probability maps illustrating the effect of the cataract

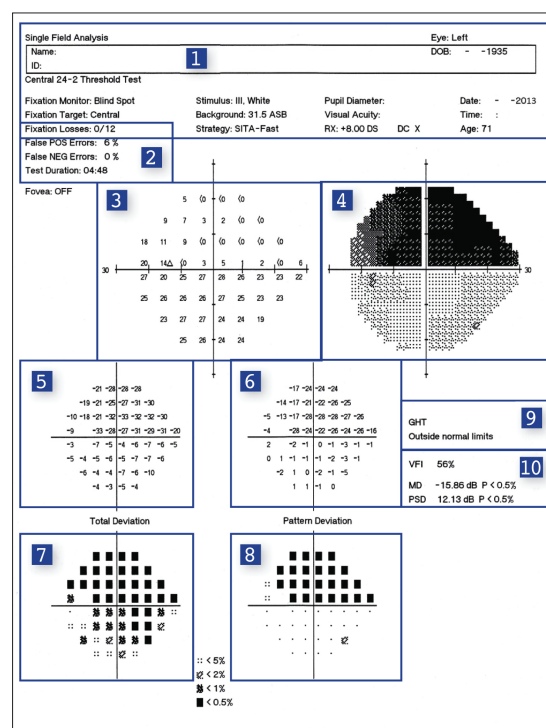


Figure 8 Single field printout of the visual field recorded with the SITA Fast algorithm and Program 24-2 of the Humphrey Field Analyzer (HFA) for the left eye of a patient with a nuclear cataract and glaucoma. Note the difference in the appearance of the Total and Pattern Deviation probability maps illustrating the effect of the cataract



results in a greater distance between the pupil centre and the Purkinje image. The outcome is displayed two dimensionally (amplitude of movement against time to occurrence) on the monitor of the perimeter in near real time and on the printout. An upward deflection represents an eye movement and a downward deflection a loss of the infrared image through lid closure, pre-corneal tear film disruption etc (Figure 9). However, it should be noted that the amplitude of the upward deflection is truncated at 10°, ie an eye movement of 10° is indistinguishable from that of, say, 20°.

If the responses to any one type of catch trial fall outside the normal limits, an 'xx' is printed alongside the given result.

The test duration is given in minutes and seconds. A prolonged test duration suggests that the patient may have had difficulty in understanding the requirements of the examination and/or sustaining concentration.

Is the field Normal?

If a **Defect** is present, what type of defect is it?

The type of **Defect** is then **Evaluated** to confirm whether it is compatible with the signs and symptoms of the patient.

The correct answer to each of these questions depends upon a number of factors including an expert understanding of the various statistical procedures for the representation of the visual field; upon a sound knowledge of the physiological variability associated with the estimate of the threshold, both in the normal and in the diseased eye; and upon feedback from the perimetrist on the performance of the patient during the examination.

The various methods of representing sensitivity are outlined below.

Numeric display - absolute values of sensitivity

The numeric values of sensitivity are displayed in the numeric display (3). The blind spot, indicated by a triangle, is situated at approximately 15° eccentricity in the temporal field.

Grey scale

The grey scale (4) provides a graphical representation of the differential light sensitivity at each stimulus location, and interpolates for the value of sensitivity between locations. In the case of the HFA, the system uses 10 shades of grey to represent the complete range of sensitivity values, with eight of the 10 shades each representing an interval

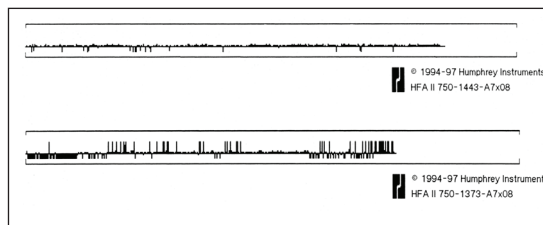


Figure 9 Printout of the results of the gaze tracker from a patient with 'good' fixation (Top) and from a patient exhibiting major difficulties in sustaining fixation (Bottom)

of 5dB. A value of 0dB is represented by black and a value of ≥41dB by white. The grey scale is not corrected for the decline in sensitivity with increase in eccentricity, which is more pronounced superiorly, and, therefore, the normal grey scale is usually lighter centrally than peripherally and usually darker superiorly than inferiorly. It is also not corrected for the decline in sensitivity with increase in age, which is greater peripherally than centrally, and, therefore, in the case of the normal visual field, the grey scale appears darker as the age of the patient increases, particularly at the edges.

Total Deviation plot

The numerical values (5) represent the difference in dB between the measured value of sensitivity at each stimulus location and the age-corrected normal value of sensitivity contained within the database of the perimeter. In the case of the HFA, a negative sign indicates that the measured value of sensitivity is lower (ie worse) than the expected age-corrected normal value.

Pattern Deviation plot

The numerical values (6) represent the difference in dB between the measured value of sensitivity at each stimulus location and the age-corrected normal value of sensitivity contained within the database of the perimeter, after having corrected for (ie removing) any overall difference in the height of the visual field from that of the normal (that arising, for example, either from a cataract, a small pupil, a 'significant' corneal opacity or an incorrect refractive correction). The correction in the height of the visual field is known as the General Height Adjustment. In the case of the HFA, the magnitude is defined as the value of the seventh most positive or least negative difference between the measured sensitivity and the age-corrected normal value of sensitivity across the 51 Total Deviation values corresponding to the Program 24-2 format (the sensitivity derived at the 52nd location, 9° immediately below the blind spot, is omitted).

Although not displayed on the printout, the General Height Adjustment can be estimated by comparing the difference between the Total and Pattern Deviation values at any given location (the difference, itself, may vary by 1dB between locations due to the mathematical rounding of either the measured and/or the age-corrected normal thresholds to integer values displayed on the printout).

Total and Pattern Deviation Probability Analysis plots

The Total Deviation and the Pattern Deviation values at each stimulus location are expressed in terms of the statistical probability (7 and 8, respectively) of the given deviation lying within the range encountered in the age-corrected normal population. The shade of the pixel representing the given statistical probability darkens as the likelihood decreases of the deviation being encountered within the normal range (expressed as a *p* value). This is the most useful part of the report: the statistical procedure permits the identification of overall (Total Deviation) and localised (Pattern Deviation) abnormalities of the visual field, respectively.

The presence and significance level of a given individual pixel on the Pattern Deviation probability plot should be viewed in conjunction with the others in terms of their spatial relationship and diagnostic position, ie a nasal step, an arcuate defect, an homonymous quadrantanopia etc.

The grey scale is of little clinical value in the evaluation of early visual field loss since it can appear normal in the presence of an obvious defect by Pattern Deviation probability analysis (Figure 10). In cases of severe loss, the General Height Adjustment cannot be calculated with any certainty and, therefore, with the HFA, the Pattern Deviation map is not displayed on the printout. In such instances, the grey scale is more useful.

Glaucoma Hemifield Test

The Glaucoma Hemifield Test (9) provides a linguistic description of the appearance of the visual field, based upon a comparison of the number and severity of the Pattern Deviation probability symbols between the superior (top) and inferior (bottom) halves of the field. The test is applicable only to the results of patients with suspected or manifest glaucoma. It is totally unsuitable for the evaluation of patients with homonymous quadrantanopia or hemianopia etc.



The visual field indices

The three visual field indices (10), Mean Deviation (MD), Pattern Standard Deviation (PSD) and Visual Field Index (VFI) each provide a quantitative summary measure of a given aspect of the visual field. If the magnitude of the MD or PSD falls outside the normal range, the appropriate statistical probability value is indicated next to the particular index. The values, themselves, of the indices are of little diagnostic use but are more useful for the assessment of progressive disease.

Mean Deviation (MD)

The Mean Deviation indicates the average overall difference in the height of the patient's visual field from that of the age-corrected normal field. The index is weighted such that the sensitivity recorded in the more central locations exerts a greater influence than that recorded at the more peripheral locations. It becomes more negative as the overall field worsens. However, it is adversely influenced by such factors as cataract and inappropriately corrected refractive error.

Pattern Standard Deviation (PSD)

The Pattern Standard Deviation indicates the difference in the shape of the patient's visual field from that of the age-corrected normal field, ie the extent of the localised, or focal, abnormality. In advanced field loss, the magnitude of the PSD is no longer representative of the damage (ie as the field loss becomes more widespread, the amount of pure localised loss becomes less).

Visual Field Index (VFI)

The Visual Field Index is relatively resistant to the effects of cataract. It approaches (but cannot be greater than) 100 per cent in normal fields and is 0 per cent in perimetrically blind patients, ie those who are unable to see the size III stimulus at the maximum luminance at any location. The index is weighted to reflect the greater importance of the paracentral regions of the field. It is essentially a staging index, ie an index to document the time course of progressive loss, but can be useful for indicating to the patient the severity of their field loss.

Case Number 3

The patient in Figure 8 has primary open-angle glaucoma in the left eye, together with a nuclear sclerotic cataract. He was examined with the SITA Fast algorithm and Program

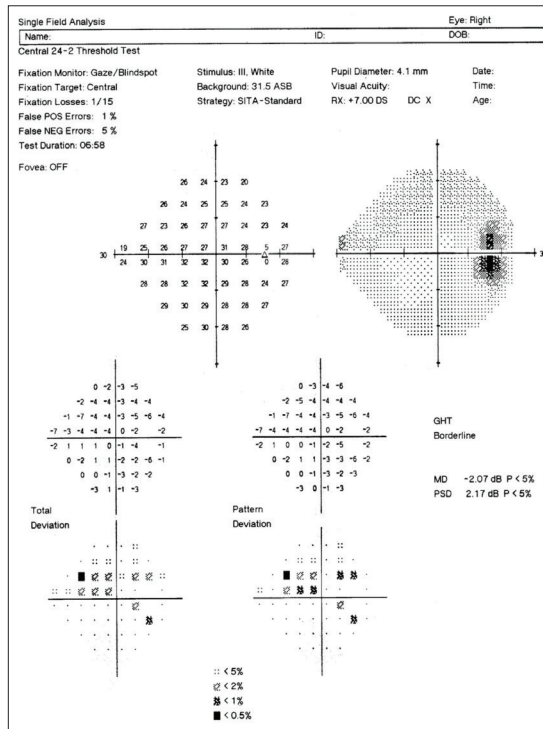


Figure 10 Single field printout of the visual field recorded with the SITA Standard algorithm and Program 24-2 of the HFA for the right eye of a patient with glaucoma. The paracentral/early arcuate defect present in the Pattern Deviation probability map is not evident in the grey scale or in the output of the Glaucoma Hemifield Test. Age-corrected suprathreshold perimetry with the HFA, at least, would not detect the presence of the field loss

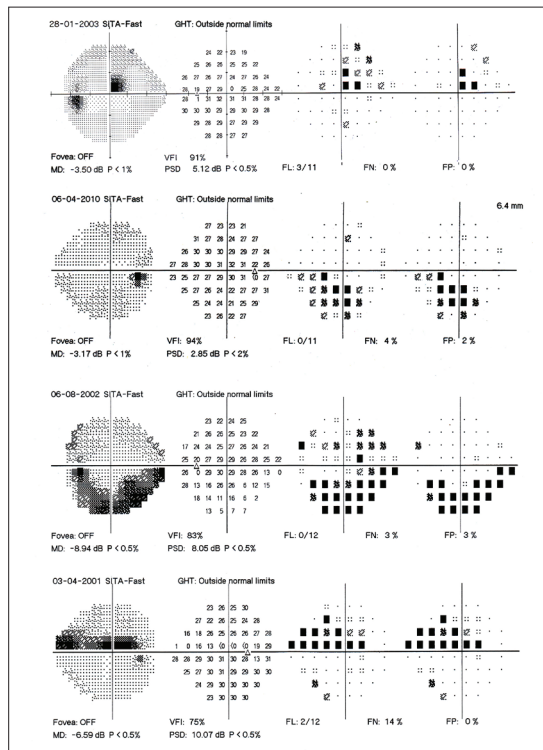


Figure 11 The grey scale, numeric values of sensitivity, and the Total and Pattern Deviation probability maps for four different cases of glaucomatous field loss. The steep sided and absolute paracentral defect illustrated in the top case is frequently associated with normal tension glaucoma

24-2 using a +8.00DS trial lens which incorporated the appropriate correction for the viewing distance of the perimeter bowl (1). The response to each of the three types of catch trials (2) indicates that a reliable response was obtained. The values of sensitivity in the numerical display indicate severe loss in the superior hemifield, which is absolute to the Goldmann size III stimulus at each of nine locations superior nasally (indicated by <0). The grey scale (4) reflects the severity of the loss in the superior field. The Total Deviation values (5), but more particularly the Total Deviation probability levels (6) illustrate the superior hemifield loss but also suggest that all but one of the stimulus locations in the inferior field exhibit a sensitivity which lies outside the age corrected normal range at a value of $p \leq 0.05$. This latter abnormality is not readily visible in the grey scaling of the inferior field. The General Height, estimated from the difference between the Total (5) and the Pattern Deviation values (7) is approximately -4dB, ie there is an overall reduction in the height of the visual field from the age-corrected normal height. This reduction is mostly, if not all, attributable to the nuclear sclerosis (it is hotly debated as to whether glaucoma produces generalised/ diffuse loss in addition to focal loss). Adjusting for the reduction in height, ie by adding approximately 4dB to each of the Total Deviation values removes the adverse influence of the cataract and highlights the glaucomatous loss as evidenced by the Pattern Deviation values (7) and by the Pattern Deviation probability map (8). In this instance, the appearance of the Pattern Deviation probability map is compatible with that of the grey scale. The outcome of the Glaucoma Hemifield Test (9) confirms the impact of the severe superior altitudinal defect, as do the Visual Field Index, the Mean Deviation and the Pattern Standard Deviation (10).

Examples of various types of glaucomatous visual field loss are given in Figure 11.

Combined structure and function probability evaluation

The need to assess, concomitantly, both structure and function in glaucoma underlines the importance of the simultaneous evaluation of the outcomes from OCT and from perimetry and such an approach is very topical.¹⁷⁻¹⁸ One example of software which enables the simultaneous evaluation of the outcomes from the ►

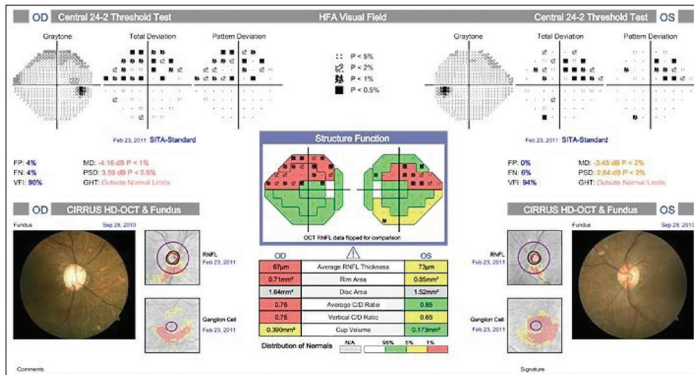


Figure 12 FORUM Glaucoma Workplace combined 24-2/30-2 and RNFL Report for a patient with glaucoma exhibiting a superior arcuate defect in each eye. Note the strong association between the retinal nerve fibre layer thickness probability levels and the Pattern Deviation probability levels

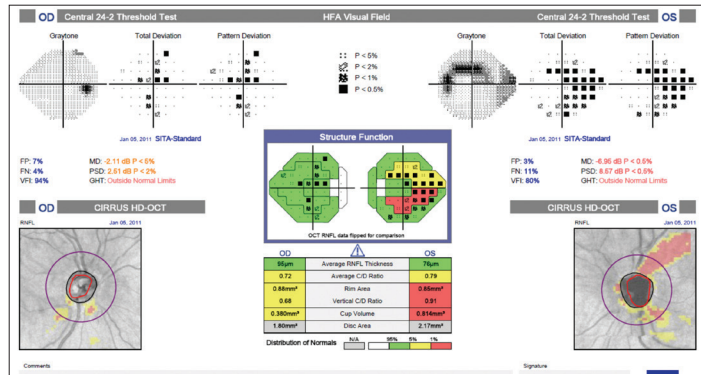


Figure 13 FORUM Glaucoma Workplace combined 24-2/30-2 and RNFL report for a patient with glaucoma exhibiting arcuate defects in both hemifields of the left eye and a paracentral visual field defect in the right eye. Note the strong association between the retinal nerve fibre layer thickness probability levels and the Pattern Deviation probability levels in the left eye. The visual field loss in the right eye is present with a seemingly normal retinal nerve fibre layer

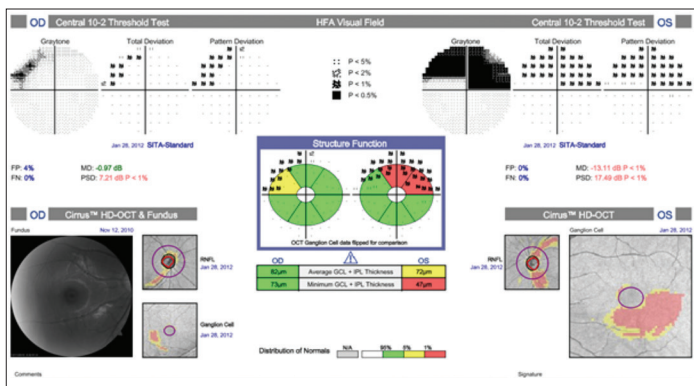


Figure 14 FORUM Glaucoma Workplace combined Program 10-2 and macular ganglion cell/inner plexiform layer thickness report for a patient with glaucoma. Note the strong association between the structural and functional outcomes

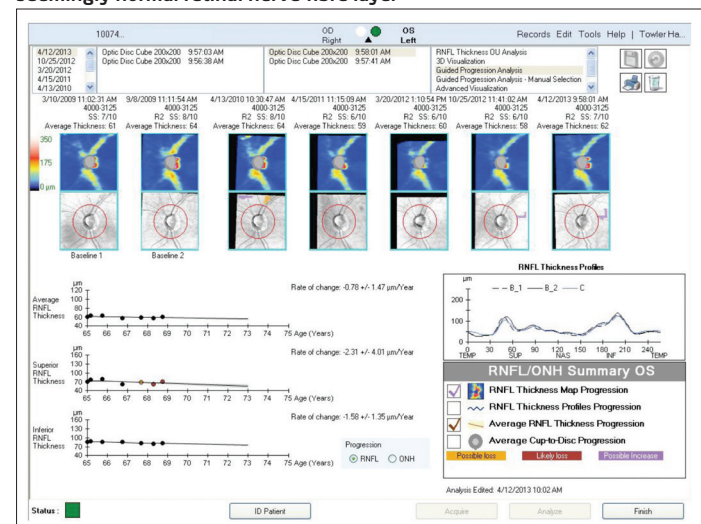


Figure 15 The Guided Progression Analysis in the left eye for a glaucoma suspect illustrating the en-face RNFL Thickness and the RNFL Thickness Change maps and the slopes of the average, superior, and inferior RNFL thicknesses, derived from the 200x200 optic disc cube, over the follow-up period

Cirrus HD-OCT with that of the HFA is FORUM Glaucoma Workplace.

The inverted en-face topographical distribution of the retinal nerve fibre layer thickness, represented in probability levels, overlaying the Pattern Deviation probability levels of Program 24-2, is shown in the centre of Figure 12 for a patient with glaucoma. The superior arcuate defect in each eye by Pattern Deviation probability analysis is clearly associated with an attenuated RNFL. The same type of plot is shown in Figure 13 for a patient with glaucoma, which is more advanced in the left eye. The optic nerve head parameters in the right eye each exhibit borderline abnormality ($p < 0.05$); however, functional abnormality appears before structural abnormality of the peripapillary RNFL thickness.

Similarly, the topographical distribution of the macular ganglion cell/ inner plexiform layer complex thickness, as a probability level, overlaying the Pattern Deviation probability levels of Program 10-2

(which thresholds 68 locations with a 2° separation out to 9° eccentricity) for another patient with glaucoma is shown in the centre of Figure 14.

FORUM Glaucoma Workplace is an advanced glaucoma management tool, and is an optional module for FORUM; a Zeiss data management system. FORUM is able to store dicom files from Zeiss and other manufacturers' diagnostic instruments.

FORUM Glaucoma Workplace also brings an added dimension to the detection and management of glaucoma. The interactive software enables the practitioner to interrogate the various datasets in order to optimise the clinical decision making at any given visit. An example of such utility is the interactive Guided Progression Analysis (Figures 15 and 16) which is separately applicable to the outcomes of OCT and of perimetry (but, currently, the interactive version is only commercially available for the latter). The software evaluates the given outcome over the follow-up period and references it to the initial/

base line examinations. The baseline can be changed at the intervention of the practitioner, for example, to assess the outcome of any change in therapy (Figure 16).

Anterior chamber angle assessment

In addition to the optic nerve head and posterior pole applications of OCT, most OCT instruments also enable a viewing of the anterior chamber angle (Figure 17).

Summary

The advantage of a combined evaluation of structural and functional outcomes, defined in terms of probability evaluation, in the diagnosis and management of glaucoma is clear. The ability to interrogate accompanying

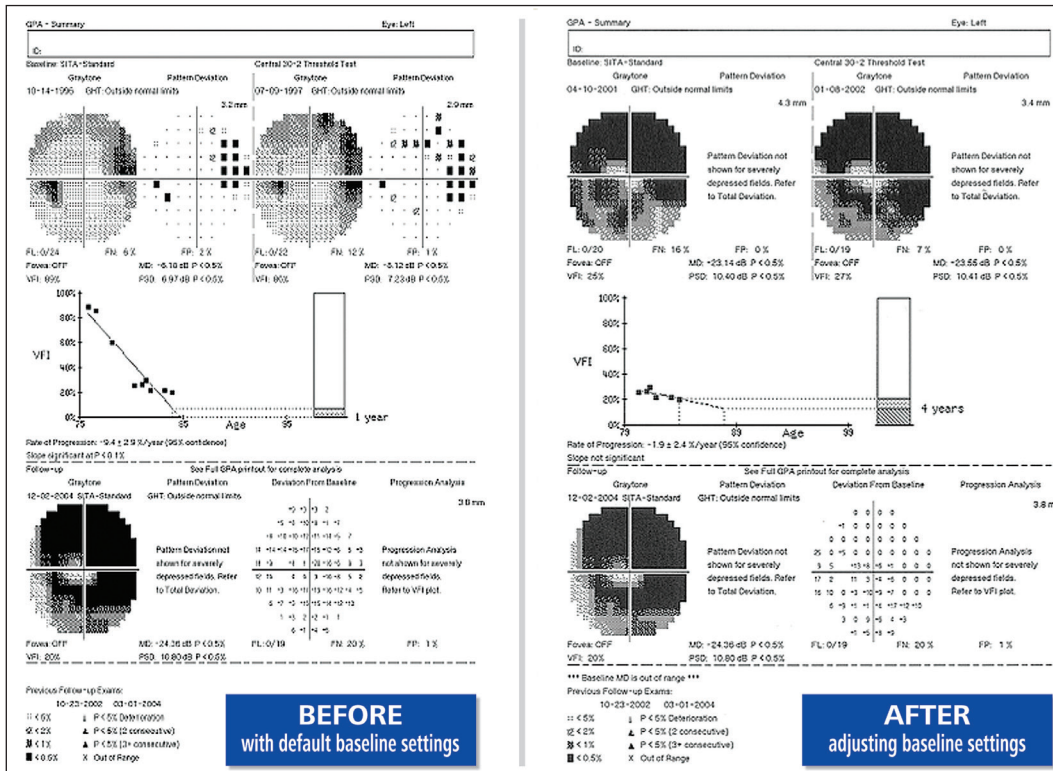


Figure 16 The Guided Progression Analysis for the visual field in the left eye of a patient with glaucoma. Top left: the visual field at the initial two examinations. Bottom left and bottom right: the final visual field of the series recorded approximately eight years after the first examination. Middle left: The marked progressive loss as evidenced by the decline in the VFI over time. Top right: The visual field at the two immediate examinations following change in therapy. Middle right: the arrest of the progression in the visual field is clearly evidenced by the outcome of the VFI referenced to the new baseline at the time of the change in therapy

software to enhance the decision making process is also apparent.

It is surely inevitable that high resolution imaging techniques will eventually replace the traditional ophthalmoscopic techniques in the assessment of glaucoma, at least. It is also likely that imaging of the anterior chamber angle will also supersede that of gonioscopy. ●

References

- 1 Quigley HA. Glaucoma. *Lancet*, 2011; 377:1367-1377.
- 2 Weinreb RN, Aung T; Medeiros FA. The pathophysiology and treatment of glaucoma: A review. *Journal of the American Medical Association*, 2014;311:1901-1911.
- 3 Keltner JL, Johnson CA, Anderson DR, et al. Ocular Hypertension Treatment Study Group. The association between glaucomatous visual fields and optic nerve head features in the Ocular Hypertension Treatment Study. *Ophthalmology*, 2006;113:1603-1612.
- 4 Miglior S, Zeyen T, Pfeiffer N, et al. Results of the European Glaucoma Prevention Study. *Ophthalmology*, 2005;112:366-375.
- 5 Malik R, Swanson WH, Garway-Heath DF. Structure-function relationship in glaucoma: past thinking and current concepts. *Clinical and Experimental Ophthalmology*, 2012;40:369-380.
- 6 Airaksinen PJ, Tuulonen A, Werner EB. Clinical evaluation of the optic disc and retinal nerve fibre layer. In: *The Glaucomas Basic Sciences* 2nd Edition. Eds Ritch R, Shields B and Krupin T. Mosby Year Book, St Louis, Missouri 1996.

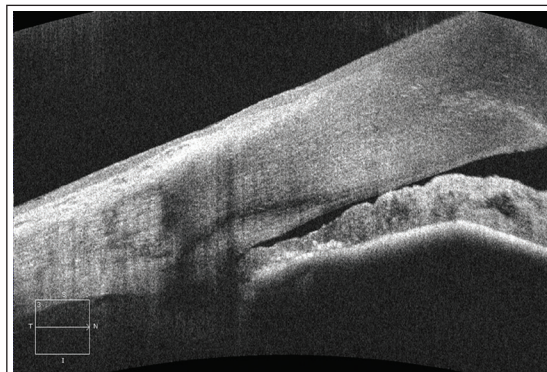


Figure 17 The Cirrus HD-OCT 500 image of the anterior chamber of a patient with a narrow angle

- 7 Hood DC, Slobodnick A, Raza AS, et al. Early glaucoma involves both deep local, and shallow widespread, retinal nerve fiber damage of the macular region. *Invest Ophthalmol Vis Sci*, 2014;55:632-649.
- 8 Zhang C, Tatham AJ, Weinreb RN, et al. Relationship between ganglion cell layer thickness and estimated retinal ganglion cell counts in the glaucomatous macula. *Ophthalmology*, 2014 [Epub ahead of print].
- 9 Quigley HA, Dunkelberger GR, Green WR. Chronic human glaucoma causing selectively greater loss of large optic nerve fibers. *Ophthalmology*, 1988;95:357-363.
- 10 Johnson C A. Selective versus non-selective losses in glaucoma. *Journal of Glaucoma*, 1994;3:S32-34.
- 11 Morgan JE, Uchida H, Caprioli J. Retinal ganglion cell death in experimental glaucoma. *British Journal of Ophthalmology*, 2000;84:303-10.
- 12 Quigley HA, Dunkelberger GR, Green

WR. Retinal ganglion cell atrophy correlated with automated perimetry in human eyes with glaucoma. *American Journal of Ophthalmology*, 1989 15;107:453-464.

- 13 Harwerth RS, Wheat JL, Fredette MJ, Anderson DR. Linking structure and function in glaucoma. *Progress in Retina and Eye Research*, 2010; 29:249-271.
- 14 Medeiros FA, Zangwill LM, Anderson DR, et al. Estimating the rate of retinal ganglion cell loss in glaucoma. *American Journal of Ophthalmology*, 2012; 154: 814-824.
- 15 Olsson J, Bengtsson B, Heijl A, Rootzen H. An improved method to estimate frequency of false positive answers in computerized perimetry. *Acta Ophthalmologica Scandinavica*, 1997;75:181-183.
- 16 Bengtsson B, Heijl A. False-negative responses in glaucoma perimetry: indicators of patient performance or test reliability? *Investigative Ophthalmology and Visual Science*, 2000; 41:2201-2004.
- 17 Bizios D, Heijl A, Bengtsson B. Integration and fusion of standard automated perimetry and optical coherence tomography data for improved automated glaucoma diagnostics. *BMC Ophthalmology*, 2011;11:20.
- 18 Raza AS1, Zhang X, De Moraes CG, et al. Improving glaucoma detection using spatially correspondent clusters of damage and by combining standard automated perimetry and optical coherence tomography. *Investigative Ophthalmology and Visual Science*, 2014;55: 612-224.

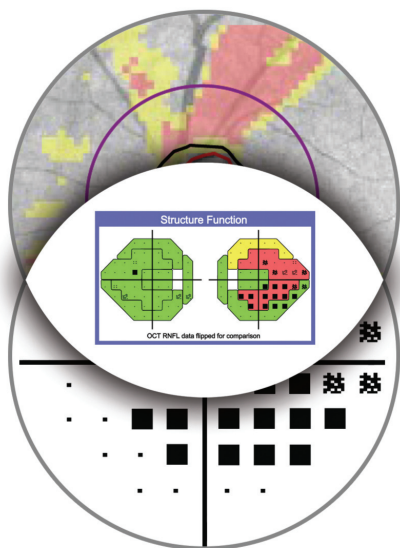
● **Professor John Wild** is Professor of Clinical Vision Sciences at Cardiff University and Honorary Research Fellow at the University Hospital of Wales

The moment you are certain it is glaucoma.
This is the moment we work for.

Available as part of our
CIRRUS HD-OCT
Humphrey Field Analyser
 new lens rebate scheme



// FORUM GLAUCOMA WORKPLACE
 MADE BY ZEISS



CIRRUS OCT + HUMPHREY

The gold standard for structure and function

ZEISS empowers you to manage the challenges of glaucoma diagnosis:

- Structure and Function Combined Reports
- Guided Progression Analysis™ (GPA™) for both structure and function
- Test results when and where you need them

Call today for more information on **FORUM Glaucoma Workplace**



www.zeiss.co.uk

Tel: 01223 401 450

customercare.uk@zeiss.com

We make it visible.